Sensitivity of quasi-dynamic topographic wetness index to choice of DEM resolution, flow routing algorithm, and soil variability

Thao T. M. Nguyen and **John P. Wilson**
GIS Research Laboratory
University of Southern California
Los Angeles, California, USA
{thaotngu, Jpwilson}@usc.edu

Abstract—**The steady-state topographic wetness index, which is frequently used to predict soil water content and sources areas for saturated overland flow, relies on two terrain attributes whose values have been shown to vary with both the grid resolution and flow routing algorithm that are used. A quasi-dynamic index (QD-TWI) has been proposed to help overcome the steady-state assumption that is implicit in the traditional form and not applicable in most semi-arid and arid landscapes. Few studies have examined the sensitivity of this index to variations in inputs and this paper examines its sensitivity to simulated DEM error, choice of DEM resolution and flow routing algorithm, and the variability of soil parameters for four small catchments in Dane County, Wisconsin.**

Keywords: quasi-dynamic topographic wetness index; sensitivity analysis; error propagatio

I. BACKGROUND

The steady-state topographic wetness index proposed by Beven and Kirby (1979) and O'Loughlin (1981) is commonly used as an indicator of soil moisture and source areas for saturated overland flow. A large body of work has examined the sensitivity of this index to the choice of grid resolution and/or flow routing algorithm (e.g. Quinn et al. 1991, Holmgren 1994, Wolock and McCabe 1995, Desmet and Govers 1996, Sauliner et al. 1997, Wilson et al. 2000). The results show that coarser grid resolutions lead to larger values and reliance on multiple vs. single flow routing algorithms produces larger values across a range of grid resolutions.

Barling et al. (1994) has since proposed a quasi-dynamic topographic wetness index (QD-TWI) that produces more realistic soil moisture predictions in certain landscapes. This index utilizes two soil (saturated hydraulic conductivity and effective porosity) and one climate parameter (flow duration or time since last precipitation event) in addition to the slope and upslope contributing area terms used in the steady-state index to account for the varying speed of soil moisture redistribution across different landscape elements. QD-TWI has been used to map wet areas and/or landslides in recent years (e.g. Duan and Grant 2000, Fried et al. 2000, Chirico et al. 2001, Gritzner et al. 2001, Borga et al. 2002). However, the initial form of this index relied on the D8 flow routing algorithm and we know little about its sensitivity to the choice of grid resolution, flow routing algorithm, and variations in soil characteristics (Wilson and Gallant 2000, Chiroco et al. 2003).

This paper aims to fill this gap by calculating the QD-TWI in four adjacent catchments to describe the sensitivity of the computed index values to the choice of grid resolution and flow routing algorithm, variation in soil characteristics, and potential errors present in the Digital Elevation Models (DEMs) that were used.

II. DATA AND METHODOLOGY

A. *Study Area and Data Preprocessing*

Four small catchments with different soil characteristics in the northwest quadrant of the 1:24K USGS Black Earth map quadrangle in Dane County, Wisconsin were chosen as study sites (Table 1).

TABLE I. STUDY AREA CHARACTERISTICS

Variables Catchments	Variables Catchments			
	#1	**#2**	**#3**	**#4**
Area (ha)	226	424	154	132
Elevation (m)	298	316	285	296
Range (m)	104	99	102	44
Roughness	2.89	2.27	2.64	2.83
Slope (%)	19.5	15.3	17.8	17.7
No. of soil map units	18	49	13	16
Mean area of map units (ha)	28	12	34	30
Sat. hydraulic conductivity (mm/h)	16.4	9.1	28.4	10.0
Effective porosity (g/cm^3)	0.74	0.51	0.47	0.70

Slope and upslope contributing area were computed from USGS DEMs with resolutions of 10-, 30-, and 90-m. The entire map quadrangle was used to avoid edge effects and small depressions were removed with the method of Jenson and Domingue (1988). Flow directions and upslope contributing areas were computed with the steepest descent (D8; O'Callaghan and Mark 1984), random single decent (Rho8; Fairfield and Leymaire 1991), multiple flow with aspect (D∞; Tarboton 1997), multiple flow direction (MFD; Quinn et al. 1991, 1995), and modified MFD (mMFD; Qin et al. 2007) flow routing algorithms.

Saturated hydraulic conductivity and effective porosity for the top 20 cm were extracted from the 1:24K SSURGO database and the flow duration was arbitrarily set to 100 days.

These particular values were chosen to set an upper threshold for soil moisture redistribution between precipitation events and to represent shallow soils in which flow is impeded by a layer with low permeability and a slope which is parallel to that of the land surface.

Catchment #3 is used as the reference throughout the paper because it had the smallest number of relatively large soil map units (i.e. the most uniform soil characteristics).

B. Quasi-Dynamic Topographic Wetness Index

According to Barling et al. (1994), the effective upslope contributing area of grid cell per unit length of contour for a specific period is:

$$a(t) = A_e = \sum_{i=1}^{n} \frac{A_i}{b} \tag{1}$$

where n is the number of upslope cells and A_i is the area of element i contributing to the subsurface drainage. The upslope area can be evaluated as:

$$A_i = \int_{s_i}^{0} b(s)ds \tag{2}$$

$$s_i = \frac{\eta(t - t_{i-1})}{K_s \tan\beta} \tag{3}$$

where $b(s)$ is the element width as a function of flow path length down the element s, s_i is the flow path for element i, η is the effective porosity, t is the drainage time and t_i and t_{i-1} are the times for all elements draining to cells i and i–1 ($t_{i-1} < t < t_i$), respectively; K_s is the saturated hydraulic conductivity; and tan β is the slope of the land surface.

C. Sensitivity Analysis

The sensitivity analysis was conducted in four stages. We first determined the number of days required to replicate the steady-state index in each of the four catchments since these results provide a first glimpse of the variability of QD-TWI by flow routing algorithm and catchment type. The QD-TWI values were next divided into five equal classes (quintiles) and the values in specific cells used to compare the spatial patterns generated from one flow routing algorithm and/or grid resolution to the next. The class limits computed with the 10 m DEM and D8 flow routing algorithm were treated as reference values and the Kappa Index used to measure the agreement between pairs of maps. We later used the same basic approach to confirm that the aforementioned effects were repeated with the 30 and 90 m DEMs, and that the differences were most pronounced in catchment #2 which contained the greatest soil variability.

D. Monte Carlo Error Propagation

We used the Monte Carlo method, which is frequently employed in environmental modelling (e.g. Oksanen and Sarjakoski 2005) with a random process that relied on the assumption of a local normal distribution (across a 5x5 cell window) to generate 500 realizations of the 10 m DEM with error. We then explored the sensitivity of the QD-TWI values generated with the five flow routing algorithms to depict the sensitivity of QD-TWI to potential elevation errors.

III. RESULTS AND DISCUSSION

A. Drainage Times

The drainage time in (2) represents the flow duration or elapsed time between consecutive rainfall events. Table 2 reports the time required for QD-TWI to match the steady-state values at the catchment outlet for each flow routing algorithm and catchment. The results show that: (a) D8 and D∞ took the least time to achieve the steady state result in two of four catchments; (b) MFD took the most time in all four catchments – at least three times longer than one or more of the D8, Rho8 and D∞ algorithms and nearly twice as long as mMFD; and (c) the desired outcome was achieved relatively quickly in catchment #3 and slowly in catchment #2 irrespective of the flow routing algorithm used. Notwithstanding the fact that the predicted times span multiple years and no account is taken of the non-linear impacts of additional precipitation events and evapo-transpiration, these results do reflect the magnitude and distribution of both topographic and soil characteristics in individual catchments.

TABLE II. TIME FOR QD-TWI TO REACH STEADY-STATE

Catchment	Time (days)				
	D8	*Rho8*	*D∞*	*MFD*	*mMFD*
1	2867	3225	2760	10678	6137
2	3157	3542	3840	11691	6662
3	1258	1490	743	3963	2428
4	2712	3035	3170	9044	5245

The PDFs in Figure 1 show steadily increasing QD-TWI values with increasing intervals between precipitation events and greater variances with coarser grid resolutions. However, the distributions of QD-TWI values are very different from the steady-state case, especially for the 10 m DEM and D8 and Rho8 single-flow routing algorithms

B. Sensitivity of QD-TWI to Flow Routing Algorithm Used

Whilst the aforementioned results give a clear indication that QD-TWI varies tremendously with the choice of flow routing algorithm, they give little indication of the spatial patterns.

Figure 2 shows the variability of QD-TWI across catchment #3 and Table 3 lists the Kappa Index values for each of the 10 pairwise comparisons. The latter indicates that mMFD produced a very different spatial pattern than the other flow routing algorithms and how generally there was little agreement among the maps generated with the different algorithms. Similar results (not shown here) were generated across all three grid resolutions and all four catchments.

C. Sensitivity of QD-TWI to Grid Resolution Used

The cumulative frequency plots (Figure 3) show how QD-TWI increased as the grid spacing was relaxed from 10 to 90 m irrespective of the flow routing algorithm that was used. These results are similar to those from earlier studies reporting larger steady state index values for multiple- vs. single-flow routing algorithms and coarser grid resolutions.

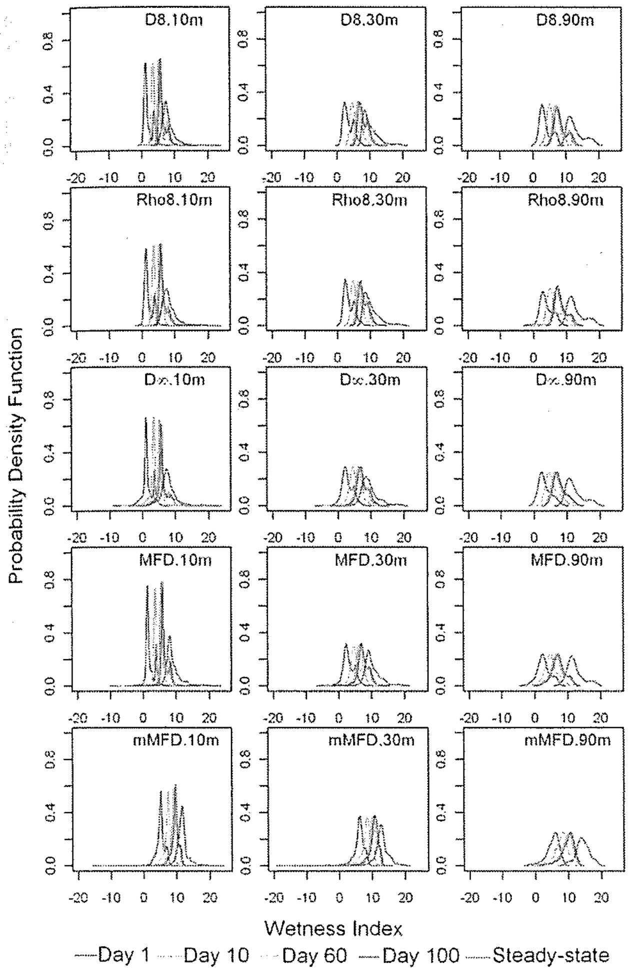

Figure 1. Probability density functions for wetness indices computed with different grid resolutions, flow routing algorithms and time intervals in catchment #3

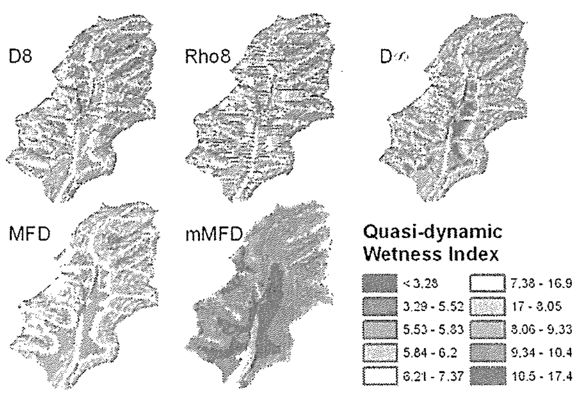

Figure 2. QD-TWI maps generated for catchment #3 using the 10 m DEM, 100 days and five flow routing algorithms

TABLE III. KAPPA INDEX VALUES FOR PAIRWISE COMPARISONS USING THE 10 M DEM IN CATCHMENT #3

	D8	Rho8	D∞	MFD	mMFD
D8	–				
Rho8	0.573	–			
D∞	0.350	0.341	–		
MFD	0.445	0.413	0.377	–	
mMFD	0.012	0.010	0.017	0.020	–

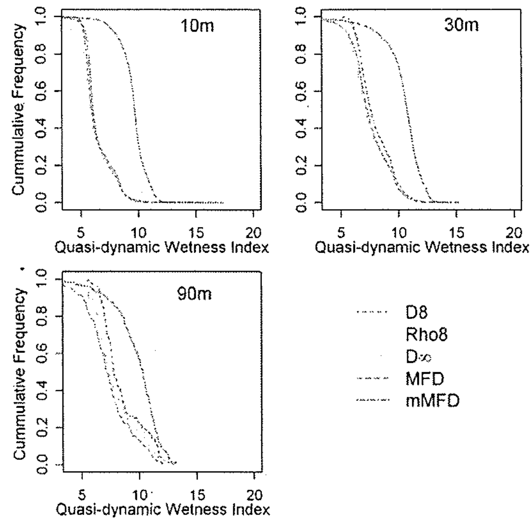

Figure 3. QD-TWI cumulative frequency distributions for catchment #3

D. *Sensitivity of QD-TWI to Changes in Soil Variability*

Table 4 summarizes the mean QD-TWI values by flow routing algorithm and catchment. These results confirm earlier ones – notably that mMFD and D∞ routinely return the largest and smallest QD-TWI values, respectively and the final row shows how the catchment with the greatest soil variability (#2) contained the maximum differences (as indicated by the lowest average Kappa Index values).

TABLE IV. MEAN QD-TWI AND KAPPA INDEX VALUES

Flow Routing Algorithm	Catchments			
	#1	*#2*	*#3*	*#4*
D8	5.68	4.92	5.51	4.72
Rho8	5.71	4.92	5.54	4.72
D∞	5.44	4.50	5.28	4.31
MFD	5.78	4.98	5.60	4.77
mMFD	8.89	7.88	8.69	7.92
Kappa Index	0.227	0.176	0.256	0.209

IV. ERROR PROPAGATION

The Monte Carlo simulation results (Table 5) demonstrate the sensitivity of computed QD-TWI values to elevation errors. These results also show how the Root Mean Square Error (RMSE) of the elevation surface increased with grid spacing, the RMSE of the QD-TWI surface declined as the grid spacing was relaxed, the MFD flow routing algorithm is the least sensitive at the 10 and 30 m resolutions (as expected), and mMFD is the most sensitive across all three grid resolutions. These results point to a complex series of relationships between terrain attributes and potential error that varies with grid spacing.

TABLE V. RMSE OF ELEVATION AND QD-TWI (500 ITERATIONS)

Catchment	10 m					
	Elev	*D8*	*Rho8*	*D∞*	*MFD*	*mMFD*
1	1.564	1.828	1.832	1.798	1.573	2.336
2	1.425	1.841	1.842	1.791	1.568	2.198
3	1.579	1.900	1.901	1.899	1.597	2.295
4	1.636	1.824	1.825	1.776	1.565	2.316
	30 m					
	Elev	*D8*	*Rho8*	*D∞*	*MFD*	*mMFD*
1	2.266	1.930	1.933	1.884	1.610	2.270
2	2.059	1.937	1.937	1.884	1.607	2.133
3	2.155	2.000	2.000	1.954	1.615	2.209
4	2.190	1.920	1.920	1.867	1.600	2.227
	90 m					
	Elev	*D8*	*Rho8*	*D∞*	*MFD*	*mMFD*
1	2.894	2.085	2.093	2.064	1.749	2.059
2	2.489	1.901	1.905	1.865	1.600	1.836
3	2.810	1.971	1.971	1.932	1.632	1.975
4	2.691	2.032	2.037	2.016	1.719	1.969

V. CONCLUSIONS

This paper extends our understanding of the sensitivity of QD-TWI to both the presence of DEM errors and soil variability as well as the choice of grid spacing and flow routing algorithm. The results show how QD-TWI is different than the steady-state index in terms of its magnitude and spatial pattern. In addition, the QD-TWI values are very sensitive to elevation errors (similar to the steady-state index). There are also substantial variations in both the magnitude and spatial patterns depending on the flow routing algorithm that is chosen. Finally, the grid spacing is important as well because coarser DEMs will eventually gloss over the topographic features that help to shape the soil moisture patterns and the hydrologic response of the catchment (irrespective of how the terrain analysis was performed).

REFERENCES

Barling, R. D., Moore, I. D. and Grayson, R. B. (1994). A quasi-dynamic wetness index for characterizing the spatial distribution of zones of surface saturation and soil water content. *Water Resources Research.* 30, 1029-1044.

Beven, K. J. and Kirkby, M. J. (1979). A physically based, variable contributing area model of basin hydrology. *Hydrological Sciences Bulletin.* 24, 43-69.

Borga, M., Dalla, F. G. and Cazorzi, F. (2002). Analysis of topographic and climatic control on rainfall-triggered shallow landsliding using a quasi-dynamic wetness index. *Journal of Hydrology.* 268, 56 - 71.

Chirico, G. B., Grayson, R. B., Longobardi, A., Villani, P. and Western, A. W. (2001). Shallow landlside hazard mapping based on a quasi-dynamic wetness index. In F. Ghassemi (Ed.) *MODSIM 2001: International Congress on Modelling and Simulation* (pp. 931– 936), Canberra, Australia: Modelling and Simulation Society.

Chirico, G. B., Grayson, R. B. and Western, A. W. (2003). On the computation of the quasi-dynamic wetness index with multiple-flow direction algorithm. *Water Resources Research.* 39, 1115-1122.

Desmet, P. J. J. and Govers, G. (1996). Comparison of routing algorithms for digital elevation models and their implications for predicting ephemeral gullies. *International Journal of Geographical Information Science.* 10, 311-331.

Duan, J. and Grant, G. E. (2000). Shallow landslide delineation for steep forest watersheds based on topographic attributes and probability analysis. In J. P. Wilson and J. C. Gallant (Eds.) *Terrain analysis: Principles and applications* (pp. 311 –329). ew York: John Wiley and Sons.

Fairfield, J. and Leymaire, P. (1991). Drainage networks from grid digital elevation models. *Water Resources Research.* 27, 709-717.

Fried, J. S., Brown, D. G., Zweifler, M. O. and Gold, M. A. (2000). Mapping contributing area for storm water discharge to streams using terrain analysis. In J. P. Wilson and J. C. Gallant (Eds.) *Terrain analysis: principles and applications* (pp. 183-204). New York: John Wiley.

Gritzner, M. L., Marcus, W. A., Aspinall, R. and Custer, S. G. (2001) Assessing landslide potential using GIS, soil wetness modeling and topographic attributes, Payette River, Idaho. *Geomorphology.* 37, 149–165.

Holmgren, P. (1994). Multiple flow direction algorithms for runoff modelling in grid based elevation models: An empirical evaluation. *Hydrological Processes.* 8, 327-334.

Jenson, S. K. and Domingue, J. O. (1988). Extracting topographic structure from digital elevation data for geographic information systems analysis. *Photogrametric Engineering and Remote Sensing.* 54, 1593-1600.

O'Callaghan, J. F. and Mark, D. M. (1984). The extraction of drainage networks from digital elevation data. *Computer Vision, Graphics and Image Processing.* 28, 323–344.

O'Loughlin, E. M. (1981). Saturation regions in catchments and their relations to soil and topographic properties. *Journal of Hydrology.* 53, 229–246.

Oksanen, J. and Sarjakoski, T. (2005). Error propagation analysis of DEM-based drainage basin delineation. *International Journal of Remote Sensing.* 26, 3085-3102.

Qin, C., Zhu, A.-X., Pei, T., Li, B., Zhou, C. and Yang, L. (2007). An adaptive approach to selecting flow partition exponent for multiple flow direction algorithm. *International Journal of Geographical Information Science.* 4, 443-458.

Quinn, P. F., Beven, K. J., Chevallier, P. and Planchon, O. (1991). The prediction of hillslope flow paths for distributed hydrological modeling using digital terrain models. *Hydrological Processes.* 5, 59-79.

Quinn, P. F., Beven, K. J. and Lamb, R. (1995). The ln (a/tanb) index: How to calculate it and how to use it within the topomodel framework. *Hydrological Processes.* 9, 161-182.

Sauliner, G.-m., Obled, C. and Beven, K. (1997). Analytical compensation between DTM grid resolution and effective values of saturated hydraulic conductivity within the topmodel framework. *Hydrological Processes.* 11, 1331-1346.

Tarboton, D. G. (1997). A new method for the determination of flow directions and upslope areas in grid digital elevation models. *Water Resources Research.* 33, 309-319.

Wilson, J. P. and Gallant, J. C. (2000). Secondary topographic attributes. In J. P. Wilson and J. C. Gallant (Eds.) *Terrain Analysis: Principles and Applications* (pp. 87– 131). New York: John Wiley and Sons.

Wilson, J. P., Repetto, P. L. and Snyder, R. D. (2000). Effect of data source, grid resolution and flow routing method on computed topographic attributes. In J. P. Wilson and J. C. Gallant (Eds.) *Terrain analysis: principles and applications* (pp. 133-61). New York: John Wiley and Sons.

Wolock, D. M. and McCabe, G. J. J. (1995). Comparison of single and multiple flow direction algorithms for computing topographic parameters in TOPMODEL. *Water Resources Research.* 31, 1315–1324.